RNA (2001), *7*:233–241. Cambridge University Press. Printed in the USA.

The *Bacillus subtilis* RNase P holoenzyme contains two RNase P RNA and two RNase P protein subunits

XING-WANG FANG,[1] XIAO-JING YANG,[1] KENNETH LITTRELL,[2] S. NIRANJANAKUMARI,[3] P. THIYAGARAJAN,[2] CAROL A. FIERKE,[3] TOBIN R. SOSNICK,[1] and TAO PAN[1]

[1]Department of Biochemistry and Molecular Biology, University of Chicago, Chicago, Illinois 60637, USA
[2]Argonne National Laboratory, Argonne, IL 60439, USA
[3]Department of Chemistry, University of Michigan, Ann Arbor, Michigan 48109, USA

ABSTRACT

Ribonuclease P (RNase P) catalyzes the 5′ maturation of precursor tRNA transcripts and, in bacteria, is composed of a catalytic RNA and a protein. We investigated the oligomerization state and the shape of the RNA alone and the holoenzyme of *Bacillus subtilis* RNase P in the absence of substrate by synchrotron small-angle X-ray scattering and affinity retention. The *B. subtilis* RNase P RNA alone is a monomer; however, the scattering profile changes upon the addition of monovalent ions, possibly suggesting different interdomain angles. To our surprise, the X-ray scattering data combined with the affinity retention results indicate that the holoenzyme contains two RNase P RNA and two RNase P protein molecules. We propose a structural model of the holoenzyme with a symmetrical arrangement of the two RNA subunits, consistent with the X-ray scattering results. This (P RNA)$_2$(P protein)$_2$ complex likely binds substrate differently than the conventional (P RNA)$_1$(P protein)$_1$ complex; therefore, the function of the *B. subtilis* RNase P holoenzyme may be more diverse than previously thought. These revisions to our knowledge of the RNase P holoenzyme suggest a more versatile role for proteins in ribonucleoprotein complexes.

Keywords: oligomerization, ribozyme, RNase P, SAXS

INTRODUCTION

The holoenzyme of a bacterial RNase P is a ribonucleoprotein complex containing an RNA component (P RNA) of ~330–420 nt and a protein component (P protein) of ~120 amino acids (Frank & Pace, 1998; Altman & Kirsebom, 1999). The functional role of the protein component in the RNase P holoenzyme has been investigated extensively (Guerrier-Takada et al., 1983, 1984; Gardiner et al., 1985; McClain et al., 1987; Reich et al., 1988; Peck-Miller & Altman, 1991; Svard & Kirsebom, 1992; Tallsjo & Kirsebom, 1993; Liu & Altman, 1994; Crary et al., 1998; Kurz et al., 1998; Loria et al., 1998; Niranjanakumari et al., 1998a, 1998b; Loria & Pan, 1999). The *Bacillus subtilis* RNase P holoenzyme is remarkably efficient in the catalysis of precursor tRNA substrates with a k_{cat}/K_m near the diffusion limit (Kurz et al., 1998; Reich et al., 1988). In the absence of the protein component, k_{cat}/K_m decreases by 10^4-fold under physiological conditions (Kurz et al., 1998). A principal effect of the P protein function has been postulated to be the enhancement of substrate binding under physiological conditions (Crary et al., 1998; Kurz et al., 1998; Niranjanakumari et al., 1998b).

The physical state of the RNase P holoenzyme has received less attention. Previous work by the Altman group conclusively showed that the *Escherichia coli* holoenzyme has an equal molar amount of RNA and protein (Talbot & Altman, 1994a). The affinity of the P protein binding to P RNA has been estimated to be ~0.5 nM, assuming a simple two-component binding isotherm (Talbot & Altman, 1994b). Functional studies by the Fierke group showed that the RNA–protein stoichiometry of the *B. subtilis* holoenzyme is also 1:1 (Niranjanakumari et al., 1998a). Most studies in this area have focused on the details of P RNA–P protein interactions using chemical modification (Vioque et al.,

Reprint requests to: Tao Pan, Department of Biochemistry and Molecular Biology, University of Chicago, 920 East 58th Street, Chicago, Illinois 60637, USA; e-mail: taopan@midway.uchicago.edu.

Abbreviations: Holoenzyme: the complex between P RNA and P protein at 1:1 molar ratio. I_0: scattering intensity at zero angle. M1 RNA: The *E. coli* RNase P RNA. P protein: The *B. subtilis* RNase P protein. P_{32P}: P RNA labeled with α-^{32}P-CTP. P_{biotin}: P RNA with a biotin covalently attached to its 3′ end. P RNA: The *B. subtilis* RNase P RNA. SAXS: small-angle X-ray scattering.

1988; Talbot & Altman, 1994b; Loria et al., 1998; Biswas et al., 2000) or spectroscopic methods (Gopalan et al., 1997, 1999). Compared to the P RNA alone, the addition of the P protein induces significant protection against hydroxyl radical attack or chemical modification in several regions in the P RNA.

To our knowledge, all of the previous work has assumed that the holoenzyme contains one P RNA and one P protein and that P RNA in the absence of P protein is a monomer. Identification of the oligomerization state of the holoenzyme will affect interpretations of the structural and functional aspects of the P protein and P protein/P RNA binding site.

This work demonstrates that in contrast to the previous assumption, the *B. subtilis* RNase P holoenzyme contains two P RNA and two P protein subunits in the absence of substrate. This conclusion is based on the results obtained from two independent methods. We use small-angle X-ray scattering (SAXS) to show that P RNA alone is a monomer and that P RNA dimerizes upon the addition of an equal molar concentration of P protein. SAXS data also suggest that the $(P\ RNA)_2(P\ protein)_2$ complex is more symmetrical than the P RNA monomer. We also use avidin beads to detect a "heterodimer" consisting of the P protein plus a nonradioactive, biotinylated P RNA and a radioactive, nonbiotinylated P RNA. The formation of the holoenzyme dimer has likely not been observed previously due to the drastic change in the shape of the P RNA in the presence and absence of the P protein that should significantly alter the mobility of the holoenzyme using size-exclusion or gel-shift methods. The formation of the holoenzyme dimer may significantly affect the binding of substrates.

RESULTS

Small-angle X-ray scattering

The oligomerization state and the shape of the *B. subtilis* RNase P holoenzyme are determined by synchrotron SAXS (Fig. 1). The high flux of the synchrotron radiation permits the measurement to be carried out at micromolar P RNA concentrations in a few seconds. Two SAXS-derived parameters are used to deduce the oligomerization state of P RNA in the absence and presence of the P protein, the scattering intensity at zero angle (I_0) and the pair distance distribution (P(r); Cantor & Schimmel, 1980). I_0 is directly proportional to the molecular weight of the complex, whereas P(r) is the sum of all distance pairs within the complex. In the absence of the P protein, the I_0 ratio (5.6 ± 0.6) of P RNA and yeast $tRNA^{Phe}$ at the same weight concentration (0.1–1 mg/mL) is proportional to their molecular weight ratio (5.4). Yeast $tRNA^{Phe}$ has been shown conclusively to be mono-dispersed under these conditions (Fang et al., 2000). Hence, this result shows that P RNA in the absence of P protein is a monomer under our experimental conditions.

Other studies have demonstrated that the P protein in the absence of the P RNA is also a monomer. Analytical ultracentrifugation experiments show that the P protein alone is a monomer under comparable conditions as the SAXS studies (S. Niranjanakumari & C.A. Fierke, unpubl. data). Similarly, the crystal structure of the P protein is consistent with the P protein being a monomer (Stams et al., 1998).

SAXS results indicate that the *B. subtilis* holoenzyme contains two P RNA molecules. The I_0 of the P RNA–

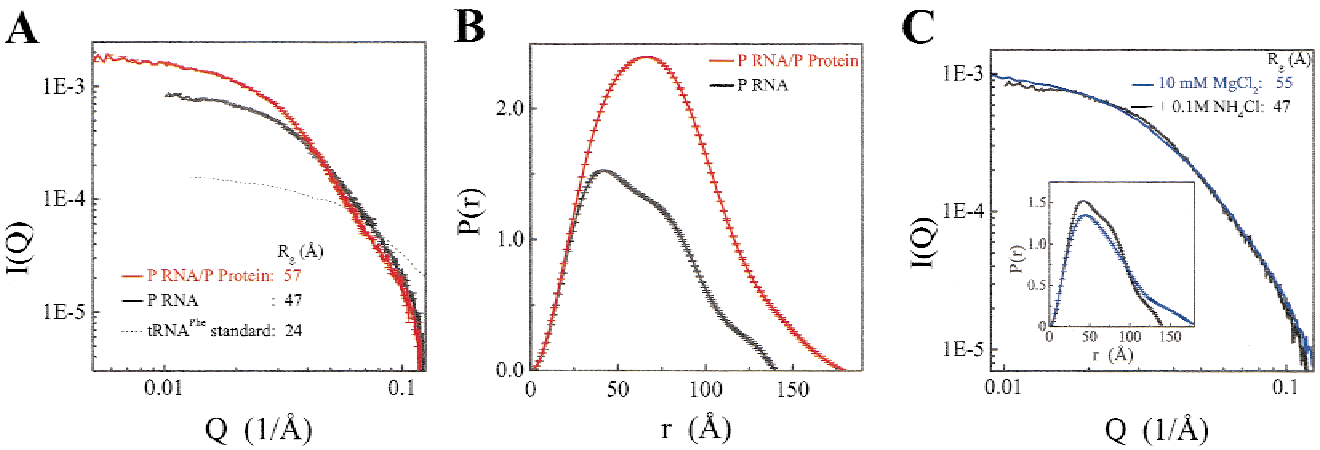

FIGURE 1. Small-angle X-ray scattering of P RNA with and without P protein. **A**: Scattering profile of P RNA with (red trace) and without (black trace) P protein in 20 mM Tris-HCl, pH 8, 10 mM $MgCl_2$, 0.1 M NH_4Cl, 0.3 mg/mL RNA (2.4 μM), 37 °C. The unmodified yeast $tRNA^{Phe}$ is used as a monomer standard (Fang et al., 2000). **B**: P(r) functions of P RNA and the holoenzyme. **C**: Scattering of P RNA with (black trace) or without (blue trace) 0.1 M NH_4Cl. The P(r) functions are shown in the insert.

P protein complex reconstituted at 1:1 RNA–protein, $(1.7 \pm 0.2) \times 10^{-3}$, is twofold higher than the I_0 of P RNA in the absence of the P protein, $(0.9 \pm 0.1) \times 10^{-3}$ (Fig. 1A). The scattering profiles cross over at high Q, consistent with oligomerization of P RNA in the holoenzyme. Because P RNA is ~10 times heavier than P protein and RNA has an approximately fivefold higher X-ray scattering signal than protein, the observed I_0 is almost entirely derived from the scattering from P RNA. The P(r) function of the holoenzyme has two times more distance pairs compared to those of the P RNA alone, as expected for the formation of a complex containing two P RNA molecules (Fig. 1B).

On the basis of the previous determination of the 1:1 stoichiometry of the P RNA and P protein in the holoenzyme under similar conditions (Talbot & Altman, 1994a; Niranjanakumari et al., 1998a), we conclude that the *B. subtilis* holoenzyme contains two P RNA and two P protein subunits. The concentration of P RNA used in the SAXS experiments ranges from 0.12–0.5 mg/mL or 1–4 μM. These concentrations lie within the range of those used in the studies of catalytic activity and stability of the holoenzyme.

Interestingly, the scattering profile of P RNA without the P protein shows considerable variation in the absence and the presence of monovalent ions, 0.1 M NH_4Cl (Fig. 1C) or 0.1 M KCl. In contrast, this concentration of monovalent ions has no effect on the scattering profile of the holoenzyme, although the dimerization decreases at higher concentrations of monovalent ions (data not shown). The native structure of P RNA is composed of two independently folding domains that are connected through two phosphodiester bonds (Loria & Pan, 1996; Fang et al., 1999). The variation in the scattering data of the P RNA monomer at different solution conditions may be explained by a difference in the relative orientation of the two domains (see Discussion).

Affinity retention

A second method, independent of SAXS, further confirms that the RNase P holoenzyme dimerizes (Fig. 2A,C). This method directly measures the formation of a heterodimer of P RNA in the presence of the P protein. In this heterodimer, one P RNA con-

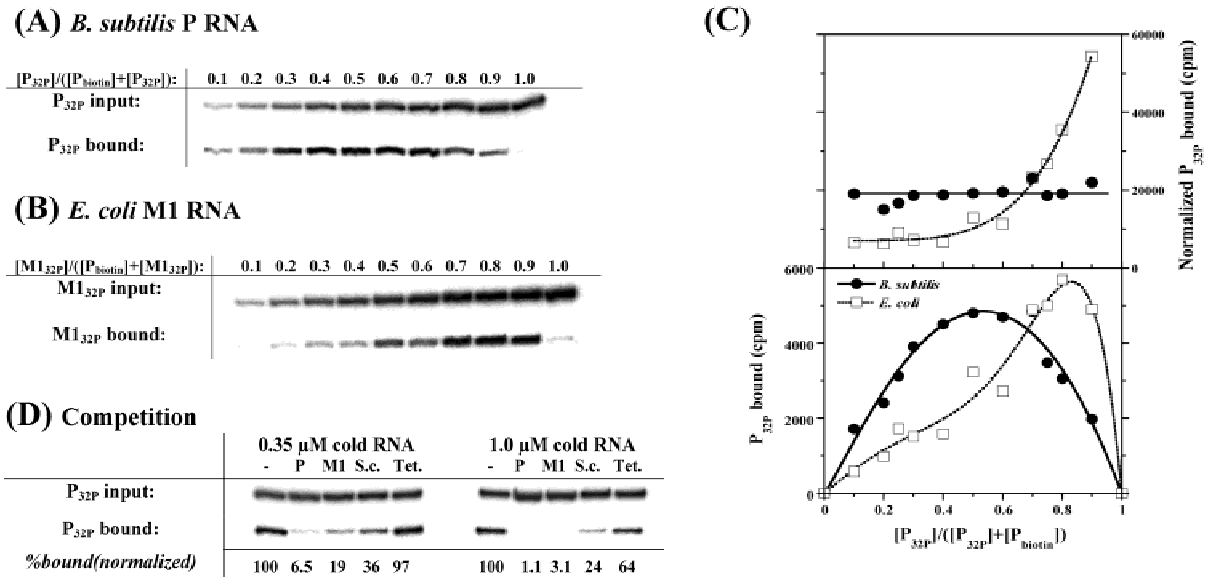

FIGURE 2. Affinity retention of P_{32P} (**A**) and radioactively labeled *E. coli* M1 RNA (**B**) with P_{biotin} and *B. subtilis* P protein. The relative amount of P_{32P} or $M1_{32P}$ input (top) and the amount of P_{32P} or $M1_{32P}$ retained on the avidin bead (bottom) are shown. The input is always more than the output and is shown at a lower contrast to better visualize the differences between each sample. No P_{32P} or $M1_{32P}$ was retained in the absence of the P protein (not shown). **C**: Bottom: the amount of P_{32P} or $M1_{32P}$ retained (y axis) is plotted against the ratio of P_{32P} or $M1_{32P}$ input (x axis). The plot of P_{32P} is described by Eq. 3a. The plot of $M1_{32P}$ can be described by Eq. 3b, however, with only four variables due to the quality of data, two constants (A_i in Eq. 3b) and two exponentials (i in Eq. 3b). The best fit for the $M1_{32P}$ data has $i_1 \sim 1$ ($A_1 \sim 7{,}500$) and $i_2 \sim 6$ ($A_6 \sim 80{,}000$). This result suggests that the $M1_{32P}$-P_{biotin} complexes contain anywhere between one to six $M1_{32P}$ molecules. Top: The amount of P_{32P} or $M1_{32P}$ retained is normalized to the fractions of P_{32P} and P_{biotin} ($y = (P_{32P}\ \text{bound}) * ([P_{32P}] + [P_{biotin}])^2/([P_{32P}] * [P_{biotin}])$). For a dimer of P RNA, this plot is a straight line. For higher order oligomers of M1 RNA, this plot shows curvature. **D**: Competition of dimer formation by nonradioactive RNAs. P: *B. subtilis* P RNA; M1: *E. coli* M1 RNA; S.c.: *S. cerevisiae* RNase P RNA; Tet.: *Tetrahymena* group I ribozyme. The concentrations of P_{32P}, P_{biotin}, and P protein are 0.06, 0.06, and 0.1 μM, respectively, in all experiments. The %bound (normalized) is obtained after subtracting the background of P_{32P} retention in the absence of P_{biotin}.

tains a biotin covalently attached to the 3′ end (P_{biotin}) and the other P RNA is radioactively labeled (P_{32P}). Qualitatively, only when P RNA oligomerizes in the presence of P protein can P_{32P} be retained on avidin beads in a P RNA mixture containing both P_{32P} and P_{biotin} (e.g., compare lanes 1.0 and 0.5 in Fig. 2A). Like the functional assay described previously (Niranjanakumari et al., 1998a), the affinity retention method shows that oligomerization of P RNA is complete only when the molar ratios of P RNA and P protein are equal (data not shown). In the experiment shown in Figure 2A, the total concentration of P_{32P} plus P_{biotin} is kept constant at $\sim$ 0.1 μM, whereas the fraction of P_{32P}, hence the amount of radioactivity in each sample, is varied. Quantitatively, the amount of P_{32P} retained exhibits a bell-shaped curve as a function of P_{32P} fraction (Fig. 2C, bottom) as described by Eq. 3a (below). Another way to present this result is to plot the amount of the P_{32P} retained divided by the fractions of P_{32P} and P_{biotin} (Fig. 2C, top). The constant *y* value indicates that the oligomerization state of the complex is invariant across all ratios of P_{32P} and P_{biotin}.

Specificity of P RNA dimerization

Unexpected results were obtained in the control experiments in which the *B. subtilis* P_{32P} is substituted with other radioactively labeled homologs of P RNA. The *E. coli* M1 RNA (Fig. 2B), the *Saccharomyces cerevisiae* RNase P RNA, or the catalytic domain of the *B. subtilis* P RNA (nt 240–409 + 1–85) form oligomers in the presence of the *B. subtilis* P protein and the *B. subtilis* P_{biotin} (data not shown). These "noncognate" complexes, however, have different oligomerization states than the "cognate" *B. subtilis* holoenzyme. The amount of $M1_{32P}$ retained exhibits a much more complicated curve as a function of $M1_{32P}$ fraction (Fig. 2C, bottom). This curve can be described by Eq. 3b (below) using two *i* parameters corresponding to the lower and upper limit of the number of $M1_{32P}$ molecules in the complex. The amount of the M1 RNA retained divided by the fractions of $M1_{32P}$ and P_{biotin} shows curvature, suggesting the formation of a higher order aggregate (Fig. 2C, top).

To examine the RNA specificity of oligomerization, we measured the ability of noncognate, nonradioactive RNAs to compete with the formation of *B. subtilis* RNase P holoenzyme dimer (Fig. 2D). P RNA and M1 RNA compete most effectively, followed by the *S. cerevisiae* RNase P RNA, and the *Tetrahymena* group I ribozyme competes least efficiently. The noncognate, nonradioactive RNAs could decrease the dimerization either by directly forming a P_{biotin}/P protein/noncognate RNA, a P_{32P}/P protein/noncognate RNA complex, or indirectly by forming a P protein/noncognate RNA complex, thereby decreasing the P protein concentration available to bind P RNA. By assuming the nonradioactive RNA only competes with P protein binding and not with dimerization, the relative affinity of P protein binding to P RNA and to another RNA can be estimated (Eq. 4, below). This estimate shows that the *E. coli* M1 RNA, the *S. cerevisiae* RNase P RNA and the *Tetrahymena* group I ribozyme binds $\sim$ 2-, 9-, and 32-fold weaker to the P protein. These affinity ratios using the *B. subtilis* P protein are similar to previous results of *E. coli* RNase P protein binding to other RNAs (Vioque et al., 1988; Talbot & Altman, 1994b; Gopalan et al., 1999).

In summary, these results suggest that dimerization of P RNA occurs in two steps. First, the P RNA binds to P protein to form a one RNA–one protein complex at subnanomolar affinity (Talbot & Altman, 1994a). Second, two $(P\ RNA)_1(P\ protein)_1$ complexes interact to form a specific $(P\ RNA)_2(P\ protein)_2$ complex. Under our conditions (0.1 μM total RNA and 0.1 μM total *B. subtilis* P protein), cognate *B. subtilis* P RNA–P protein complexes form dimers, whereas noncognate RNase P RNA–P protein complexes form aggregates.

DISCUSSION

Modeling the shape of the P RNA monomer and the holoenzyme dimer

The shape of the P RNA monomer and the holoenzyme is modeled and compared to the R_g and P(r) function from SAXS to gain further insight on how dimerization of P RNA may occur. Our models begin with the P RNA model proposed by Westhof and coworkers (Massire et al., 1998). The modeling is carried out in two stages. First, the P RNA monomer is modified to allow a better fit to the SAXS data (Fig. 3A). Next, two P RNA molecules are brought together and the dimer model compared to the SAXS data (Fig. 3B).

The R_g of the P RNA monomer calculated from the Westhof model of P RNA is smaller than that observed in the SAXS measurements (43 versus 47–55 Å). Consistent with the smaller R_g, the P(r) function of the Westhof model also has a narrower distribution of mass pairs than that derived from the experimental data. The P RNA in the Westhof model, however, was constructed in the context of a bound tRNA substrate that may affect the conformation of the P RNA, whereas the SAXS measurements were performed on the P RNA alone. For example, the *B. subtilis* P RNA is composed of two independently folding domains and the binding of tRNA could potentially reorient the two domains in the P RNA monomer (Loria & Pan, 1999).

We modified the Westhof model to determine whether a change in the domain orientation alone could partially account for the difference in the R_g and P(r). In our modeling, the structures of the catalytic domain (C-domain, nt 240–409 + 1–80) and the specificity do-

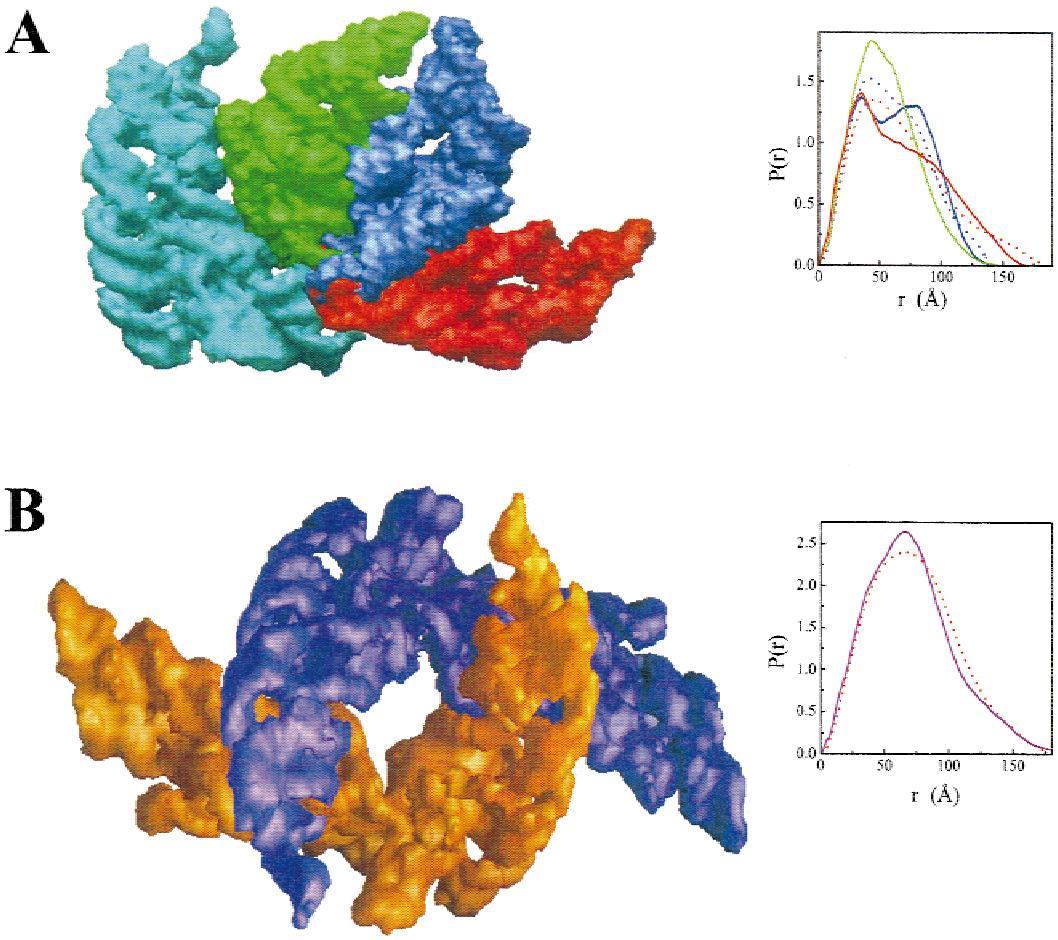

FIGURE 3. Models of the P RNA monomer and the two P RNAs in the holoenzyme dimer. **A**: P RNA monomer. The C-domain in all three models is identical and shown in light blue. The S-domain of the Westhof model (green) is rotated away to obtain a better fit to the SAXS data in the presence (dark blue) and absence (red) of 0.1 M NH_4Cl. The experimental P(r) functions are shown as dashed lines and the calculated P(r) functions are shown as solid lines. **B**: The two P RNA subunits in the holoenzyme (purple and gold). The contribution of the P protein to the scattering profile and P(r) is negligible. The P(r) (solid line) and R_g (56 Å) of the model agrees well with the experimental P(r) (dashed line) and R_g (57 Å).

main (S-domain, nt 86–239) are kept the same as those in the Westhof model. However, the domain–domain connection at the P7 and P5 helices (between nt 239 and 240) is used as a hinge and the J5.1/7 region (nt 81–85) is extended to allow the S-domain to be rotated away from the C-domain. These changes at the domain junction are consistent with biochemical studies that suggest little domain–domain interaction in the *B. subtilis* P RNA monomer (Massire et al., 1998; T. Pan, unpubl. results) and that the J5.1/7 region shows a significant conformational change upon tRNA binding (Odell et al., 1998).

Rotation of the interdomain angle from ~30° in the Westhof model (green) to ~60° (dark blue) and ~90° (red) changes the R_g for the new P RNA models from 43 Å to 47 and 53 Å, respectively. These values are much closer to the R_g of 47 and 55 Å experimentally determined in the presence and absence of 0.1 M NH_4Cl, respectively. Similarly, the P(r) functions of the models with altered domain orientations agree better with the experimental data (Fig. 3A). These models suggest that the domain orientation in the P RNA monomer is variable and dependent on the solution conditions, in particular, on the presence of monovalent salt. This conclusion provides a possible explanation for the monovalent ion dependence of the catalytic reaction carried out by the P RNA alone (Smith et al., 1992; Beebe et al., 1996).

We have also generated a model of the holoenzyme that is only meant to identify an overall shape consistent with the SAXS data. In this model, two P RNA molecules with modified interdomain orientations are brought together with the C-domain of one P RNA proximal to the S-domain of the other P RNA and vice versa (Fig. 3B). To allow a better fit to the SAXS data, the precise angle between the domains in the holoenzyme is similar (~85°), but not identical to that in either P RNA monomer model. Changing the angle between the domains should be feasible because P protein binding

could easily compensate for any potential energetic cost of altering the domain orientation. This holoenzyme model has a twofold symmetry regarding the two P RNA molecules and is significantly more compact than alternate models without the twofold symmetry (not shown). The model has similar P(r) and R_g (56 Å) to the experimentally measured P(r) and R_g (57 Å) (Fig. 3B).

Topological specificity of the P RNA dimer

The formation of the P RNA dimer in the holoenzyme is likely due to the presence of multiple RNA binding sites in the *B. subtilis* P protein. Three binding sites have been inferred from its crystal structure (Stams et al., 1998). Initially, one or more of these site in the P protein may bind one P RNA to form a specific $(P\ RNA)_1(P\ protein)_1$ complex. Subsequently, another site in the P protein in one $(P\ RNA)_1(P\ protein)_1$ complex binds the P RNA in another $(P\ RNA)_1(P\ protein)_1$ complex and vice versa. This subsequent, symmetrical binding event results in a holoenzyme containing two P RNA and two P protein molecules (Fig. 4, left).

Crosslinking and affinity cleavage data suggest that two potential RNA-binding sites, the highly conserved "RNR" motif and the metal-binding loop, interact with P RNA in the $(P\ RNA)_1(P\ protein)_1$ complex (Stams et al., 1998; Biswas et al., 2000; S. Niranjanakumari & C. A. Fierke, unpubl. results). Therefore, the best candidate for the RNA-binding site in the P protein responsible for P RNA dimerization is the same site involved in binding of the 5′ leader of a pre-tRNA substrate (Niranjanakumari et al., 1998b). This binding site in the P protein binds 4–5 single-stranded nucleotides with little sequence specificity. In the absence of substrate, this site presumably binds a single-stranded region in the P RNA. This proposed positioning of the P protein/P RNA contact in the dimer suggests that the affinity of substrates and products should be affected by dimerization.

Different oligomers form when the cognate *B. subtilis* P RNA is replaced with the noncognate, *E. coli* M1 RNA (Fig. 4, right). The initial binding of the P protein to M1 RNA or to P RNA is probably similar, as suggested in numerous studies (Guerrier-Takada et al., 1983; Reich et al., 1988; Talbot & Altman 1994a). However, due to the variation in the shape of these RNAs, the subsequent binding event probably does not occur symmetrically for the noncognate *E. coli* M1 RNA–P protein complex. Nonsymmetric interactions between $(M1\ RNA)_1(P\ protein)_1$ and $(P\ RNA)_1(P\ protein)_1$ complexes would not enable both RNAs to interact with both proteins simultaneously. Each P protein is free to interact with a third RNA, leading to aggregation, rather than to well-defined oligomeric species.

The dimerization of P RNA in the holoenzyme significantly affects the interpretation of previously published in vitro studies of the RNase P holoenzyme (Talbot & Altman, 1994a, 1994b; Loria et al., 1998; Gopalan et al., 1999; Biswas et al., 2000). Published protein–RNA affinity measurements are certainly affected by formation of a holoenzyme dimer. Furthermore, dimerization could significantly influence the interpretation of experiments designed to identify P protein-binding sites. For example, the P protein footprint on P RNA is much larger than expected for the small size of the P protein. Our data suggests that some of the footprint may be derived from intersubunit RNA–RNA interactions formed upon dimerization. Likewise, chemical crosslinking between the protein and the RNA should be reevaluated because the protein may crosslink to two different RNAs in the same complex. Finally, mutational analysis of the P protein can be complicated due to the potential effects of the mutant on either P RNA binding or P RNA dimerization.

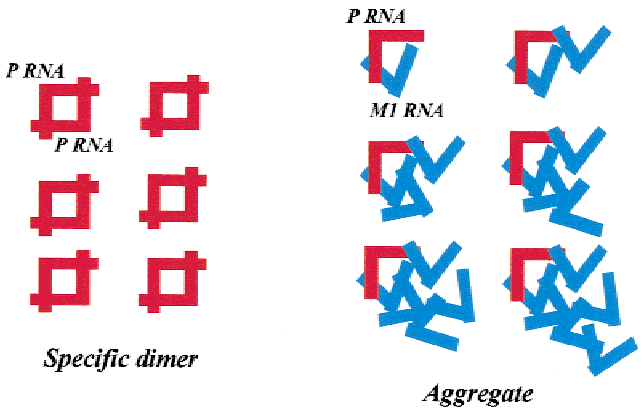

FIGURE 4. A model of the topological specificity of the *B. subtilis* holoenzyme. Binding of the 5′ leader binding site of the P protein to a putative single-stranded region in the P RNA can occur symmetrically, so that the cognate P RNA–P protein complex is a dimer. The same binding event for a noncognate RNA–P protein complex is not symmetric and both RNAs cannot bind to the same two P proteins, resulting in an aggregate.

Potential function of the P RNA dimer

Several functions can be proposed for the holoenzyme dimer, depending on the mode of substrate binding. One can envision that substrate binding may be cooperative, either by having two substrate molecules bind to the dimer or by requiring dissociation of the dimer to allow substrate binding at either site. Cooperativity of this nature could thus promote the specificity of substrate binding and/or fine-tune the regulation by increasing the sensitivity of RNase P activity to the substrate concentration. Alternatively, if the specific structure of the P RNA subunits allows binding of only one substrate molecule at a time, substrate binding may be linked to the rapid release of the tRNA product, thus facilitating the turnover of the RNase P reaction. A third potential function is the ability of the holoenzyme

to process non-tRNA substrates that require a larger binding surface. A particular example may be the *B. subtilis* homolog of the SRP RNA, which is much more like the eukaryotic version (~300 residues) than the *E. coli* 4.5 S RNA (~120 residues). Determination of the function of the holoenzyme dimer is being actively pursued in our laboratories.

MATERIALS AND METHODS

Preparation of RNA and the *B. subtilis* P protein

RNAs were obtained by standard transcription using T7 RNA polymerase (Milligan & Uhlenbeck, 1989). The *E. coli* M1 RNA was obtained from a construct described previously (Harris et al., 1994). The *S. cerevisiae* P RNA construct contained the full-length P RNA as described in Tranguch & Engelke (1993). The P protein was prepared from an overexpression clone using the protocol described previously (Niranjanakumari et al., 1998a). The concentration of the P protein was determined by dye binding using bovine serum albumin as a standard or by absorbance at 280 nm in 5 M guanidinium hydrochloride using an extinction coefficient of 5120 M^{-1} cm^{-1} (Niranjanakumari et al., 1998a). The concentration of the P RNA was determined by absorbance at 260 nm in 50 mM NH_4OAc using an extinction coefficient of 3.46×10^6 M^{-1} cm^{-1}. This extinction coefficient has been corrected for the hypochromicity effect by measuring the absorbance after complete digestion of the P RNA with nuclease P1.

Small-angle X-ray scattering

SAXS experiments were carried out at the SAXS instrument on the BESSRC ID-12 beam-line of Argonne National Laboratory's Advanced Photon Source (Seifert et al., 2000). Data were collected using a 9-element (15×15 cm) mosaic CCD area detector and exposure times were 1–6 s for each measurement. Sample to detector distance was 3 m and energy of X-ray radiation was set to 13.5 keV. Computer-controlled Hamilton brand syringes injected sample into a thermostated flow cell made of a 1.5 mm diameter cylindrical quartz capillary. The background scattering was from a buffer solution in the identical configuration. To reduce the possibility of radiation damage, samples were measured under constant flow conditions. SAXS data are presented as the scattering intensity per solid angle, I(Q), where the scattering vector Q, is defined as $4\pi \sin\theta/\lambda$, λ is the X-ray wavelength, and θ is the half scattering angle. The P(r) functions were calculated according to

$$P(r) = \frac{1}{2\pi^2} \int_{Q_{max}}^{Q_{min}} I(Q)\, Q\, sin(Q)\, dQ \qquad (1)$$

using the indirect Fourier inversion algorithms developed by Moore (1980). The R_g was determined from the second moment of P(r) according to

$$R_g^2 = \frac{\int_0^{d_{max}} r^2 P(r)\, dr}{2\int_0^{d_{max}} P(r)\, dr} \qquad (2)$$

No significant differences were observed for the R_g values determined from the P(r) analysis and Guinier analysis (data not shown).

Formation of the (P_{32P} P_{biotin})(P protein)$_2$ heteroholoenzyme

P_{32P} and other radioactively labeled RNAs were obtained by standard transcription using T7 RNA polymerase in the presence of α-^{32}P-CTP. P_{biotin} was obtained in two steps. First, N^6(aminohexyl)adenosine-5′, 3′ bisphosphate (Sigma-Aldrich, St. Louis, Missouri) was ligated to the 3′ end of the nonradioactive P RNA using T4 RNA ligase (England et al., 1980). The ligated product was extracted with phenol/$CHCl_3$ and precipitated with ethanol. Next, the RNA was redissolved in 50 mM $NaHCO_3$, pH 8.5, and 39 mg/mL sulfosuccinimidyl 2-(biotinamido)-ethyl-1,3-dithiopropionate (NHS-SS-biotin, Pierce, Rockford, Illinois). The reaction mixture was incubated at ambient temperature for 1 h and the biotinylated RNA product was purified on an 8% polyacrylamide gel containing 7 M urea.

In the affinity retention experiment, P_{32P} (or other radioactively labeled RNAs) and P_{biotin} were mixed at designated ratios after the renaturation step and prior to the addition of the P protein. The total P RNA concentration was kept constant at 0.1 μM. The holoenzyme was reconstituted as described previously (Loria et al., 1998). Briefly, the RNA mixture was heated in Tris-HCl at 85 °C for 2 min, followed by incubation at room temperature for 3 min. $MgCl_2$ was added at designated concentrations and the RNA was further incubated at 50 °C for 5 min. NH_4Cl and P protein were added and the mixture incubated at 37 °C for 2 min. The final condition was 50 mM tris-HCl, pH 7.5, 10 mM $MgCl_2$, 0.1 M NH_4Cl (buffer A) with 0.1 μM total P RNA and 0.1 μM P protein. The holoenzyme mixture (50 μL) was immediately combined with 50 μL Streptavidin paramagnetic particles (Promega, Madison, Wisconsin) preequilibrated with buffer A. After 3 min incubation at room temperature, the supernatant was removed and the particles washed with an equal volume of buffer A. The P_{32P} in the (P_{32P} P_{biotin})(P protein)$_2$ complex was eluted by the addition of 10 μL of 50 mM Tris-HCl, pH 7.5, 0.1 M NH_4Cl, 50 mM EDTA to the particles. The eluted mixture was analyzed on denaturing polyacrylamide gels.

Three types of (P RNA)$_2$(P protein)$_2$ complex are formed in the presence of P_{32P}, P_{biotin}, and P protein: (P_{32P} P_{32P})(P protein)$_2$, (P_{32P} P_{biotin})(P protein)$_2$, and (P_{biotin} P_{biotin})(P protein)$_2$. The proportion of these complexes is directly related to the fraction of P_{32P} ($[P_{32P}]/([P_{32P}] + [P_{biotin}]) = x$) and P_{biotin} ($[P_{biotin}]/([P_{32P}] + [P_{biotin}]) = 1 - x$) as x^2, $2x(1 - x)$, and $(1 - x)^2$, respectively. Only the (P_{32P} P_{biotin})(P protein)$_2$ complex is detected in the affinity retention experiment. Therefore, the amount of P_{32P} eluted (counts per minute in arbitrary unit) is a function of the P_{32P} fraction:

$$P_{32P}\ \text{bound} = A * 2 * x * (1 - x), \qquad (3a)$$

where A is a constant related to the amount of radioactivity and exposure time in each experiment. For an aggregate containing one P_{biotin} and one or multiple $M1_{32P}$, this equation can be modified to

$$M1_{32P}\ \text{bound} = \sum A_i * (1 - x) * x^i \quad (3b)$$

The relative affinity of the M1 RNA, *S. cerevisiae* RNase P RNA, and the *Tetrahymena* group I ribozyme was calculated as follows. First, the background of P_{32P} binding to the streptavidin bead in the absence of P_{biotin} was subtracted from the amount of P_{32P} bound in the presence of P_{biotin}. This amount of the holoenzyme dimer (y axis) can be expressed as a function of [nonradioactive RNA]/([P_{32P}] + [P_{biotin}]) = x according to

$$y \approx B/(1 + (K_{\text{P RNA}}/K_{\text{other RNA}}) * x)^2 \quad (4)$$

where $K_{\text{P RNA}}/K_{\text{other RNA}}$ is the relative affinity of the P protein binding to P RNA and to another RNA. B is a constant related to the amount of radioactivity and exposure time used in each experiment.

Molecular modeling

Calculations of P(r) function from predicted models were conducted using the program XTL modified for use with nucleic acids (Thiyagarajan et al., 1996). The P RNA with the extended P1 region was built based on the structural model by Westhof and co-workers (Massire et al., 1998). Seventeen nucleotides were added and extended from C4 and A395 in the helix P1 as an extending stem-loop, forming an energy-favoring continuous groove surface with the neighboring helix P19. The model was then refined by 1,000 steps of conjugate gradient refinement.

ACKNOWLEDGMENTS

This work benefitted by the use of the Advanced Photon Source and was supported by grants from the National Institutes of Health (GM52993 to T.P., GM57880 to T.P and T.R.S. and GM55387 to C.A.F.), the U.S. Department of Energy, BES Chemical and Materials Sciences under contract #W-31-109-ENG-38 to the University of Chicago, and by a University of Chicago-Argonne National Laboratory Collaborative Seed Grant Program (T.R.S. and P.T). We thank Dr. J. Piccirilli for the generous gift of the *Tetrahymena* group I ribozyme. We also thank the reviewers for their insightful comments.

Received July 14, 2000; returned for revision November 15, 2000; revised manuscript received November 20, 2000

REFERENCES

Altman S, Kirsebom L. 1999. Ribonuclease P. In: Gesteland RF, Cech TR, Atkins JF, eds. *The RNA world.* Cold Spring Harbor, New York: Cold Spring Harbor Laboratory Press. pp. 351–380.

Beebe JA, Kurz JC, Fierke CA. 1996. Magnesium ions are required by *Bacillus subtilis* RNase P RNA for both binding and cleaving precursor $tRNA^{Asp}$. *Biochemistry 35*:10493–10505.

Biswas R, Ledman DW, Fox RO, Altman S, Gopalan V. 2000. Mapping RNA–protein interactions in ribonuclease P from *Escherichia coli* using disulfide-linked EDTA-Fe. *J Mol Biol 296*:19–31.

Cantor CR, Schimmel PR. 1980. Other scattering and diffraction techniques. In: *Biophysical chemistry*. San Francisco: W.H. Freeman and Company. Ch. 14, pp 811–818.

Crary SM, Niranjanakumari S, Fierke CA. 1998. The protein component of *Bacillus subtilis* RNase P increases catalytic efficiency by enhancing interactions with the 5′ leader sequence of pre-$tRNA^{Asp}$. *Biochemistry 37*:9409–9416.

England TE, Bruce AG, Uhlenbeck OC. 1980. Specific labeling of 3′ termini of RNA with T4 RNA ligase. *Methods Enzymol 65*: 65–74.

Fang XW, Littrell K, Yang XJ, Henderson SJ, Seifert S, Thiyagarajan P, Pan T, Sosnick TR. 2000. Mg^{2+} dependent compaction of yeast tRNAPhe and the catalytic domain of the *B. subtilis* RNase P RNA determined by small-angle X-ray scattering. *Biochemistry 39*:11107–11113.

Fang XW, Pan T, Sosnick TR. 1999. A thermodynamic framework and cooperativity in the tertiary folding of a Mg^{2+}-dependent ribozyme. *Biochemistry 38*:16840–16846.

Frank DN, Pace NR. 1998. Ribonuclease P: Unity and diversity in a tRNA processing ribozyme. *Annu Rev Biochem 67*:153–180.

Gardiner KJ, Marsh TL, Pace NR. 1985. Ion dependence of the *Bacillus subtilis* RNase P reaction. *J Biol Chem 260*:5415–5419.

Gopalan V, Golbik R, Schreiber G, Fersht AR, Altman S. 1997. Fluorescence properties of a tryptophan residue in an aromatic core of the protein subunit of ribonuclease P from *Escherichia coli*. *J Mol Biol 267*:765–769.

Gopalan V, Kuhne H, Biswas R, Li H, Brudvig GW, Altman S. 1999. Mapping RNA–protein interactions in ribonuclease P from *Escherichia coli* using electron paramagnetic resonance spectroscopy. *Biochemistry 38*:1705–1714.

Guerrier-Takada C, Gardiner K, Marsh T, Pace NR, Altman S. 1983. The RNA moiety of ribonuclease P is the catalytic subunit of the enzyme. *Cell 35*:849–857.

Guerrier-Takada C, McClain WH, Altman S. 1984. Cleavage of tRNA precursors by the RNA subunit of *E. coli* ribonuclease P (M1 RNA) is influenced by 3′-proximal CCA in the substrates. *Cell 38*:219–224.

Harris ME, Nolan JM, Malhotra A, Brown JW, Pace NR. 1994. Global architecture of the ribonuclease P RNA-pre tRNA complex. *EMBO J 13*:3953–3963.

Kurz JC, Niranjanakumari S, Fierke CA. 1998. Protein component of *Bacillus subtilis* RNase P specifically enhances the affinity for precursor-$tRNA^{Asp}$. *Biochemistry 37*:2393–2400.

Liu F, Altman S. 1994. Differential evolution of substrates for an RNA enzyme in the presence and absence of its protein cofactor. *Cell 77*:1093–1100.

Loria A, Niranjanakumari S, Fierke CA, Pan T. 1998. Recognition of a pre-tRNA substrate by the *Bacillus subtilis* RNase P holoenzyme. *Biochemistry 37*:15466–15473.

Loria A, Pan T. 1996. Domain structure of the ribozyme from eubacterial ribonuclease P. *RNA 2*:551–563.

Loria A, Pan T. 1999. The cleavage step of ribonuclease P catalysis is determined by ribozyme-substrate interactions both distal and proximal to the cleavage site. *Biochemistry 38*:8612–8620.

Massire C, Jaeger L, Westhof E. 1998. Derivation of the three-dimensional architecture of bacterial ribonuclease P RNAs from comparative sequence analysis. *J Mol Biol 279*:773–793.

McClain WH, Guerrier-Takada C, Altman S. 1987. Model substrates for an RNA enzyme. *Science 238*:527–530.

Milligan JF, Uhlenbeck OC. 1989. Synthesis of small RNAs using T7 RNA polymerase. *Methods Enzymol 180*:51–64.

Moore PB. 1980. Small-angle scattering. Information content and error analysis. *J Appl Cryst 13*:168.

Niranjanakumari S, Kurz JC, Fierke CA. 1998a. Expression, purification and characterization of the recombinant RNase P protein component from *Bacillus subtilis*. *Nucleic Acids Res 26*:3090–3096.

Niranjanakumari S, Stams T, Crary SM, Christianson DW, Fierke CA. 1998b. Protein component of the ribozyme ribonuclease P alters

substrate recognition by directly contacting precursor tRNA. *Proc Natl Acad Sci USA 95*:15212–15217.

Odell L, Huang V, Jakacka M, Pan T. 1998. Interaction of structural modules in substrate binding by the ribozyme from *Bacillus subtilis* RNase P. *Nucleic Acids Res 26*:3717–3723.

Peck-Miller KA, Altman S. 1991. Kinetics of the processing of the precursor to 4.5 S RNA, a naturally occurring substrate for RNase P from *Escherichia coli. J Mol Biol 221*:1–5.

Reich C, Olsen GJ, Pace B, Pace NR. 1988. Role of the Protein moiety of ribonuclease P, a ribonucleoprotein enzyme. *Science 239*:178–181.

Seifert S, Winans RE, Tiede DM, Thiyagarajan P. 2000. Design and performance of an ASAXS instrument at the Advanced Photon Source. *J Appl Cryst 33*:782–784.

Smith D, Burgin AB, Haas ES, Pace NR. 1992. Influence of metal ions on the ribonuclease P reaction. Distinguishing substrate binding from catalysis. *J Biol Chem 267*:2429–2436.

Stams T, Niranjanakumari S, Fierke CA, Christianson DW. 1998. Ribonuclease P protein structure: Evolutionary origins in the translational apparatus. *Science 280*:752–755.

Svard SF, Kirsebom LA. 1992. Several regions of a tRNA precursor determine the *Escherichia coli* RNase P cleavage site. *J Mol Biol 227*:1019–1031.

Talbot SJ, Altman S. 1994a. Gel retardation analysis of the interaction between C5 protein and M1 RNA in the formation of the ribonuclease P holoenzyme from *Escherichia coli. Biochemistry 33*:1399–1405.

Talbot SJ, Altman S. 1994b. Kinetic and thermodynamic analysis of RNA–protein interactions in the RNase P holoenzyme from *Escherichia coli. Biochemistry 33*:1406–1411.

Tallsjo A, Kirsebom LA. 1993. Product release is a rate-limiting step during cleavage by the catalytic RNA subunit of *Escherichia coli* RNase P. *Nucleic Acids Res 21*:51–57.

Thiyagarajan P, Henderson SJ, Joachimiak A. 1996. Solution structures of GroEL and its complex with rhodanese from small-angle neutron scattering. *Structure 4*:79–88.

Tranguch AJ, Engelke DR. 1993. Comparative structural analysis of nuclear RNAse P RNAs from yeast. *J Biol Chem 268*:14045–14053.

Vioque A, Arnez J, Altman S. 1988. Protein–RNA interactions in the RNase P holoenzyme from *Escherichia coli. J Mol Biol 202*:835–848.